In-silico and In-vitro Evaluation of Novel Carboxamide Analogue on the Metastasis of Triple Negative Breast Cancer Cells Utilizing Novel PCPTC-loaded PEGylated-PLGA Nanocarriers

In-silico and In-vitro Evaluation of Novel Carboxamide Analogue on the Metastasis of Triple Negative Breast Cancer Cells Utilizing Novel PCPTC-loaded PEGylated-PLGA Nanocarriers

*,†*Ankur Sharma*[1, 2], †*Amka Nagar*[3], *Susan Hawthorne*[1] , *Mohini Singh*[3]

[1]*School of Pharmacy and Pharmaceutical Sciences, Ulster University, Cromore Road, Coleraine, Co. Londonderry, BT52 1SA, UK*

[2]*Strathclyde Institute of Pharmacy and Biomedical Sciences, University of Strathclyde, Cathedral Street, Glasgow, G4 0RE, Scotland, UK*

[3]*Department of Life Science, Sharda School of Basic Sciences and Research, Sharda University, Greater Noida, U.P, 201310, India*

*Author to whom correspondence should be addressed

† Author (s) contributed equally

Correspondence

Dr Ankur Sharma

[1]*School of Pharmacy and Pharmaceutical Sciences,*

Ulster University, Cromore Road, Coleraine,

Co. Londonderry, BT52 1SA, UK.

[2]*Strathclyde Institute of Pharmacy and Biomedical Sciences,*

University of Strathclyde, Cathedral Street,

Glasgow, G4 0RE, Scotland, UK

Asharma.nanotechnologist@gmail.com

Abstract

Aim: This study aimed to determine the effects of novel N-{3-[(pyridin-4-yl)carbamoyl] phenyl} thiophene-2-carboxamide or PCPTC chemical moiety loaded Poly(lactic-co-glycolic acid)-Poly (Ethylene glycol) or (PLGA-PEGylated) NP as an anti-metastatic Ran GTPase therapeutic agent on MDA-MB231 triple-negative human breast cancer cells.

Method: Molecular docking and MD simulation was done to determine the binding potential of novel carboxamide PCPTC with Ran GTPase. PLGA and PLGA-PEG based NP encapsulating PCPCT were fabricated using the Modified Double Emulsion Solvent Evaporation Technique and characterized for size, zeta potential, polydispersity and morphology. *In vitro* evaluation of loaded nanoparticles such as cellular localization study, cell proliferation, cell migration, cell invasion and Ran Pull Down assay were carried out on MDA-MB231 breast cancer cells. Ran downregulation was determined by pull down assay.

Results: PCPTC with Ran GTPase exhibited strong structural stability based on *in silico* analysis. The average sizes of PCPTC loaded NP ranged between 166.3 nm to 257.5 nm and were all negatively charged. Scanning electron microscopy data showed that loaded NP were smooth and spherical. Fluorescence microscopy data confirmed the intracellular localization of loaded nanoparticles inside the MDA-MB231 cells. Cell proliferation assay (MTT assay) confirmed the cytotoxic effect of the loaded-NP when compared to blank nanoparticles. PCPTC-loaded NP inhibited metastasis and invasion of MDA-MB231 cells. This anti-metastatic and the anti-invasive effect was due to the Ran GTPase cycle blockage, which was confirmed by performing Ran Pull down assay. we propose that PCPTC is a promising compound to inhibit Ran GTPase and may act as a potential therapeutic agent against breast cancer.

Conclusion: PCPTC-loaded NP successfully stopped the metastasis of MDA-MB231 cells by disrupting the Ran cycle.

Keywords: PLGA Nanoparticles, Ran GTPase, Breast Cancer, Metastasis, Invasion, RAN

1. Introduction

The anti-metastatic effect of numerous anti-cancer agents has been evaluated extensively in recent years [1]. Examples include agents such as paclitaxel, doxorubicin and genistein, which have been used widely against different cancer types [2], [3]. Although various anti-cancer or anti-metastatic agents are available clinically, there is an ongoing and pressing need to discover new anti-cancer agents that lead to better therapeutic outcomes. One obstacle that hinders the delivery of most of the anti-cancer agents is poor water solubility, leading to poor bioavailability [4]. Such considerations have prompted the investigation of nanoparticulate drug delivery systems, with documented success in enhancing bioavailability [5]. For instance, curcumin has been used experimentally as an effective anti-cancer agent and possesses poor bioavailability when used in the un-encapsulated form [6]. Solubility and bioavailability increases when encapsulated within colloidal carriers [7]

The use of novel carboxamides such as PCPTC may hold a promise in delivering an anti-metastatic effect. Study conducted by Yu-Ren Liao et.al., had shown the anti-proliferation effect of [N-(2-Dimethylaminoethyl)-4,8-dihydrobenzo (1,2-b;4,5-b') dithio-phene-2-carboxamide phosphoric acid salt in colorectal and hepatocellular cancer cells by acting on the caspase cascade-dependent signalling pathway [8].

. While exhibiting anti-proliferative activity, the carboxamide analogue had shown very mild cytotoxicity in normal cells [8] [9] (Liao Y, Lu C, Lai K, Yang J, Kuo SC, Wen Y, Fushiya S and Wu T: The novel carboxamide analogue ITR-284 induces caspase-dependent apoptotic cell death in human hepatocellular and colorectal cancer cells. Mol Med Rep 7: 1539-1544, 2013, Yang J, Lin C, Lu C, Wen Y, Tsai F and Tsai S: Carboxamide analogue ITR-284 evokes apoptosis and inhibits migration ability in human lung adenocarcinoma A549 cells. Oncol Rep 37: 1786-1792, 2017).

It is confirmed in human cell lines, such as MDA-MB231, with interference of the Ran cycle and subsequent effects on intra-nuclear and intra-cellular trafficking of biomolecules being a proposed mechanism of action [10]. The Ran cycle itself plays a vital role in molecular transportation within cells during the various cell phases and is key to their division and differentiation [10]. It is a multi-step biological pathway, governing the intra-nuclear transportation of biological molecules, with RCC1 (Regulator of chromosome condensation 1), a chromosomal regulatory protein, being an important regulatory factor [11]. RCC1 has a Ran-binding motif that helps inter-conversion of cargo-carrying Ran-GDP into active Ran-GTP and dispatch of the cargo [12]. It has been documented that the

inactivation of RCC1 motif binding sites results in the loss of RCC1, causing premature initiation of mitosis [11]. This leads to cell cycle arrest in the G1 phase [13]. In addition to this, the supply of the cargo required for the functioning of the cell cycle is stopped [13].

This study aimed to investigate the binding of PCPTC to Ran GTP and interfere with the ability of block binding with cargo-carrying Ran-GDP. This will stop the conversion of Ran-GDP into active Ran-GTP, which will stop the transportation of the cargo and conceivably arrest the metastatic potential of cancer cells, especially in therapeutically challenging diseases, such as metastatic breast cancer.

2. Materials and Methods

2.1 Materials

Poly[(d,l-lactide-co-glycolide)-*co*-PEG]diblock Resomer® RGP d 5055(5% PEG) and Resomer® RGP d 50105 (10% PEG) were obtained from by Boehringer-Ingelheim (Ingelheim,Germany). Poly(D, L-lactide-*co*-glycolide) mw 20kDa-28kDA, poly(vinyl alcohol) (PVA) 87-89% hydrolysed (MW 31 000-50 000) was purchased from Sigma Chemical Co. (St. Louis, USA). N-{3-[(pyridine-4-yl)carbamoyl]phenyl}thiophene-2-carboxamide was obtained from Molport (Illinois, USA). Coumarin-6, DAPI, ethanol, , Anti-mouse IgG alkaline phosphatase (in goat), protease inhibitor cocktail, Tween® 20 and BCIP/NBT solution were obtained from Sigma-Aldrich (Dorset, UK). MTT (3-(4, 5-dimethylthiazol-2-yl)-2, 5-diphenyl tetrazolium bromide was obtained from Thermo Fisher Scientific (Paisley, UK). The Cultrex BME Cell Invasion Assay kit was purchased from Bio-techne (Oxford, UK). Ran Activation assay kit was purchased from Generon Ltd. (Berkshire, UK). NuPAGE ® MOPS SDS Running buffer (20×), NuPAGE ® Transfer buffer (20 ×) and NuPAGE 4-12 % Bis-Tris gel 10 well were purchased from Novex, Life Technologies (Renfrew, UK). X-cell sure lock ™ Mini cell electrophoresis apparatus and See-Blue Pre-Stained Standard Marker were obtained from Invitrogen (Paisley, UK). Nitrocellulose membrane (0.1 µm) was obtained from Invitrogen™ (Hertfordshire, UK). All the other chemicals used were of appropriate analytical grade.

2.2 Methods

2.2.1 Structure preparation (protein and ligand), Docking and Pose analysis

The three-dimensional crystal structure of Ran GTPase was obtained from Protein Data Bank with PDB id 1K5G [14] resolution solved at 3.10 Å for structure-based virtual screening. The system initially contained 12 chains (A to L). Only two chains (A and B) were chosen for docking, while the remaining chains were removed. Non-standard amino acids, such as AF3 and GDP, were excluded during protein preparation by using chimera-1.14 software [15]. Moreover, the protein's structure was modified by the inclusion of polar hydrogen atoms, which play a crucial role in establishing hydrogen bond interactions with the ligand (PCPTC) to overcome the challenges throughout protein-ligand interactions.

The 3D structure of the ligand (PCPTC) was obtained from PubChem. During ligand preparation, the Mg ions and AF3 were deleted. Herein, docking was performed at Chimera in the same active pocket of Ran GTPase having grid box 15 × 15 × 15 Å and is aligned with the X, Y and Z axes. Its central coordinates are 3.22, 3.46 and -22.16.

To validate the docking procedure with PCPTC both 2D and 3D interaction images were produced using the academic Schrödinger-Maestro v12.4 suite.

2.2.2 ADMET Profiling

Furthermore, the OSIRIS [16] and Swiss ADME web tool was employed to evaluate the potential lead compound PCPTC, to derive the various characteristics such as drug similarity, pharmacokinetics, and physiochemical properties [17].

2.2.3 Explicit-solvent MD simulation

The stability of the docked complex was accessed through 100 ns explicit-water molecular dynamics (MD) simulation by using the academic version of Desmond v5.6 module in Schrödinger-Maestro academic Desmond [18].

2.2.4 PCPTC-Loaded Nanoparticle Fabrication

NP was fabricated by using a modified double emulsion solvent evaporation technique, where a water-oil-water (W/O/W) emulsion was prepared (Sharma et. al., 2021). Briefly, PLGA was dissolved in 4 ml dichloromethane (DCM) and vortexed vigorously until the polymer dissolved entirely. Thereafter, 1 ml of 2.5% (w/v) and 50 ml of 1.25 % (w/v) PVA solution was prepared as internal aqueous phase and external aqueous phase, respectively. The payload (PCPTC) was dissolved in 0.8 ml of 2.5 % (w/v) PVA and 0.2 ml of methanol.

PCPTC solution was added slowly and mixed with the solution of polymer and DCM under constant homogenisation (homogeniser-VMR VDI12 S2) at 10000 rpm for 2 minutes (W/O emulsion or primary emulsion).

The W/O primary emulsion was added dropwise and mixed with 1.25 % PVA solution (50 ml) resulting in the formation of a W/O/W emulsion (secondary emulsion) under constant homogenisation (homogeniser-Silverson L5T FAR A17122) at 10000 rpm for 6 minutes at room temperature. Samples were left overnight with constant stirring to remove the organic phase. Samples were then washed and pelleted by centrifugation (13440 G force) thrice for 10 minutes each, firstly with ultrapure water, then with 2 % sucrose solution followed by ultrapure water again. After the last centrifugation, the pellet was dispersed in 5 ml distilled water and samples were lyophilised for further use (Labconco freeze dryer, Mason technology, Missouri, USA).

2.2.5 Characterisation of PCPTC-Nanoparticles

The size, zeta potential and polydispersity index (PDI) of loaded NP were obtained using dynamic light scattering (Zetamaster Malvern instruments, UK) using a 15mW laser and an incident beam of 676 nm. A sample of NP (5 mg) was passed through a 0.45 µm filter, dispersed in distilled water and used to measure average diameter and PDI. Potassium chloride solution (1 ml, 1 mM) was used as a dispersal medium for the determination of zeta potential.

2.2.6 Encapsulation Efficiency

Determination of PCPTC encapsulation efficiency was performed using an indirect method. During the formulation of the NP, the supernatants were collected after the first centrifugation step and used to determine the encapsulated payload. Briefly, 200 µl of each sample was added to a 96-well plate. Absorbance was measured photometrically at 284 nm (FLUOstar Omega Multi-Mode microplate reader) and a standard curve (0.0 - 0.5 mg ml^{-1} PCPTC) was used to calculate concentration. Encapsulation efficiency was then determined using the standard curve. The percentage ratio of the determined PCPTC to the theoretical maximum loading was done to determine the encapsulation efficiency.

2.2.7 Drug Release Study

PCPTC release from NP was studied to determine the release properties of NP. Briefly, 5 mg of NP was suspended in 1 ml PBS (pH 7.4) for 96 hours and rotated end to end in a lab-made incubation chamber at 37 °C. After every 24 hours, 1 ml samples were centrifuged at 10 000 rpm for 10 minutes, supernatant was collected, and drug release was measured by measuring the 200 µl sample's absorbance at 284 nm using FLUOstar Omega Multi-Mode microplate reader.

2.2.8 Scanning Electron Microscopy

An ultra-thin layer of lyophilised NP powder was coated on a carbon tape metal grid. It was sputter coated with gold for 15 minutes and samples were examined using scanning electron microscopy (FEI Quanta 400 FEG) under high vacuum mode and 2° electron ETD detection.

2.2.9 Cellular Uptake of NP

Fluorescently labelled, PCTC-loaded NP was used in this part of the study. These NPs were prepared using a minor modification of the preparation procedure. Coumarin-6 was added to the DCM phase of the primary emulsion, containing polymer and PCTC, to give a final dye concentration of 1% in the oil phase. MDA-MB231 cells, a human breast cancer cell line, were seeded (1×10^5 cells) using 1 ml of media into a 2-well chamber and incubated for 24 hours (37 ^oC and 5% $CO_{2)}$. Cells were transfected by the addition of 1 µg of labelled NP dispersed in 1 ml transfection media (opti- media) and then incubated for 24 hours (37 ^oC and 5% $CO_{2)}$. After 24 hours, the medium was aspirated and cells were washed 2-3 times with PBS. Cells were then washed with 4 % paraformaldehyde twice and stained with 100 µl of 0.5 mg ml^{-1} DAPI solution. Cells were visualised using fluorescence microscopy using the DAPI channel (λ_{ex}-358nm, λ_{em}-461 nm) for visualising stained blue nucleus and the FITC (λ_{ex}-488 nm, λ_{em}-519 nm) channel was used for coumarin dye loaded PCPTC nanoparticles (Nikon Eclipse E400 Fluorescence Microscope, Nikon Y-FL, Japan).

2.2.10 Cell Viability

MDA-MB231 cells (4 x 10^4 cells per well in 1 ml medium) were seeded in 24-well cell culture plates and left to adhere overnight at 37^oC and 5% CO_2. After 24 hours, the cells were transfected with either 1.0 µg or 2.5 µg of PCPTC-loaded NP, suspended in 500 µl of media.

Cell viability was evaluated after 24, 48, 72, and 96 hours with the culture media being changed every day. Media was aspirated cells were washed with sterile PBS and media containing 500 µl of 10 mg ml^{-1} MTT dye was added to each well. All plates were incubated for 3 hours at 37 °C. After this time, the supernatant was aspirated and formazan dissolved using dimethyl sulfoxide (500 µl per well). Absorbance was measured at 570 nm (FLUOstar Omega microplate reader, Germany). Cytotoxicity was calculated as a percentage of cell growth concerning untreated cells and cells treated with blank NP.

2.2.11 Cell Migration

MDA-MB231 cells (7.5×10^5 cells per well in 2 ml medium) were seeded in 6-well plates and incubated at 37 ºC for 48 hours to allow them to become confluent. Once the cells had reached confluency, a scratch was made across the diameter of each well using a 200 µl sterile pipette tip. Cells were then transfected using either 1.0 µg or 2.5 µg of PCPTC-loaded NP dispersed in 2 ml of media. Each well was viewed using light microscopy after 0, 24, 48 and 72 hours to determine the percentage scratch closure. Data was analysed using Image J software (Cambridge, Massachusetts, USA).

2.2.12 Cell Invasion Assay-Transwell membrane Invasion

Cell invasion assay was performed using a Cultrex® 96-well BME Cell Invasion Assay kit. The assay was performed using the manufacturer's instructions. Briefly, 50 µl 1x BME solution (supplied with the kit) was added to each well of the upper chamber to cast a membrane and was incubated overnight at 37 °C. After overnight incubation, any remaining solution was aspirated and wells were seeded with 5×10^4 cells per well in 150 µl SFM. Cells were then incubated for 24 hours at 37 °C and 5 % CO_2. Cells were then transfected with 2.5 µg PCPCT in PLGA-PEG-5%-PCPTC NP in media for 24 hours and 48 hours. Complete media was added at the bottom of each chamber well, which acted as a chemo-attractant for the cells. After 48 hours, cells were washed using washing buffer (supplied with the kit) and a mixture of 12 µl calcein-AM solution and cell dissociation medium was added to each bottom chamber well to dissociate invaded cells from the bottom of the wells of upper chambers. The plate was then incubated for 30 minutes at 37 °C and fluorescence was measured (λ_{ex} 485 nm, λ_{em} 520 nm).

2.2.13 Ran Pull-down Assay

MDA-MB231 cells (1×10^5 cells per well) in 2 ml media were seeded in 6-well plates. After that cells were transfected using 2.5 µg of filtered PCPTC-PLGA-PEG-5% NP and then incubated for 48 hours. After 24 hours, the media was aspirated, and cells were washed 2-3 times with PBS. Then cells were trypsinized using 1 ml trypsin in each well and incubated at 37 ^oC with 5% CO_2 for 5 minutes. Then cells were taken out of the incubator and 1ml of growth medium was added into each well. Cells were poured into a falcon conical centrifugation tube and centrifugation was done at 1500 rpm (25 G force) for 5 minutes. The supernatant was discarded and the pellet was suspended with sterile PBS and centrifuged again at 1500 rpm (25 G force) for 5 minutes. This was repeated twice.

The protein extraction was done using a protein extraction kit as per manufacturer instructions (Sigma-Aldrich, Paisley, UK) and the Ran Pull-down assay was carried out using an appropriate protocol provided with the RAN Pull-down assay kit. Briefly, 1 ml lysate was transferred to micro-centrifugation tubes from each well and 40 µl of RanBP1 Agarose bead slurry was quickly added to each sample lysate. Lysate samples were then incubated at 4 °C for 1 hour under gentle agitation. Then samples were centrifuged at 14000 rpm (2195 G force) for 10 seconds. The supernatant was discarded carefully without disturbing the pellet and the pellet was washed thrice with 0.5 ml assay buffer with centrifugation and aspiration each time. After the final washing, 40 µl of sample buffer was added to each sample and the sample was boiled for 5-10 minutes. *SDS-PAGE*- X-cell sure lock ™ Mini cell electrophoresis apparatus was set up as per the manufacturer's instruction to run the gel. The electrophoretic tank was filled with running buffer and later 40 µl of each sample was loaded into individual wells of a NuPAGE 4-12 % Bis-Tris gel. The gel was run under 200 V and 50 mA for 50 minutes to separate the bands. *Western blotting*- The gel was blotted onto the nitrocellulose blotting membrane using the X-cell sure lock ™ blotting module as per the manufacturer's instructions. Briefly, the gel was placed under the soaked (in transfer buffer) blotting nitrocellulose membrane, sandwiched between the soaked sponges (in transfer buffer) and placed in the blot module carefully ensuring that there were no gaps or bubbles between the gel and blotting membrane. Then, the transfer buffer was added to the blot module until the gel sandwich was immersed entirely. The outer chamber of the blot module tank was filled with deionised water and the blotting of the gel was at 50 V, 200 mA for 1 hour. After the blotting, the membrane was immersed into the 5 % non-fat dry milk solution in TBST buffer for 1 hour at room temperature under mild shaking. After one hour, the solution was removed and freshly prepared primary antibody (1 in 1000) in 5 % non-fat dry

milk solution in TBST (10 ml) was added to the membrane. The immersed membrane was incubated for 2 hours under constant shaking at room temperature. After 2 hours, the solution was poured out and the membrane was washed thrice using TBST buffer (20 ml). Then, the membrane was again incubated with freshly prepared secondary antibody (1 in 30 000) diluted in 5 % non-fat dry milk solution in TBST for 1.5 hours at room temperature under constant agitation. Then membrane was washed thrice with TBST buffer for 5 minutes each. BCIP/NBT (10 ml) substrate solution was then added to the membrane to allow the development of bands. The process was stopped by extensive washing of the membrane with water. Bands were detected using Gel doc EX imager, BioRad (Hertfordshire, UK). The entire procedure was done to study the reduced expression of Ran-GTPase. Western blot was done to study the reduced expression of Ran-GTPase.

3. Results

3.1 Docking and intermolecular interaction analysis

The compound PCPTC showed -7.4 Kcal/mol binding affinity with the target protein Ran GTPase (1K5G) **(Table 1)**. PCPTC molecule exhibiting considerable docking score was selected for subsequent re-docking and intermolecular interaction analysis. The docked complex Ran GTPase-PCPTC exhibited 5 hydrophobic interactions formation (Phe^{35}, Tyr^{39}, Val^{40}, Ile^{126}, Ala^{151}) and two glycine (Gly^{20} and Gly^{22}) residues were also recorded. Notably, π- π stacking with residues (Phe^{35} and Tyr^{39}), while Lys^{152} residue exhibited π-cation interaction. Moreover, the residues (Lys^{23}, Lys^{38}, Lys^{250} and Lys^{272}) showed a positive interaction and the residue (Asp^{125}) showed one negative. Additionally, the complex also displayed five polar residues with Thr^{21}, Thr^{24}, Thr^{25}, Asn^{122} and Ser^{150} (**Figure 1, Table 2)**.

3.2 ADME & T analysis

In addition, an ADME analysis was conducted for prominent compound PCPTC by using the OSIRIS and Swiss ADME tools. From this analysis, we obtained information about the compound such as their pharmacokinetic and toxicity profiles (as detailed in **Supplementary Table 1**). From the assessment, it was observed that PCPTC followed Lipinski's rule of five and was determined to be safe for human cells, with no toxicity or carcinogenicity **(Supplementary Figure 1)**.

3.3 MD simulation analysis

In the field of drug discovery, Molecular Dynamics (MD) simulation is a computational technique used to evaluate the dynamic behaviour of protein-ligand complex. The stability and the occurrence of intermolecular interactions between protein-ligand were assessed over 100ns simulation trajectory **(Figure 2)** [19].

3.4 RMSD and RMSF analysis

RMSD values were calculated for various aspects of the protein structure, including Cα, backbone, sidechain, and heavy atoms, along with the protein fit ligand from every single frame during the 100 ns simulation trajectory. This was done to measure the average change in displacement that occurred in the docked complexes to the initial frame [19]. Cα atom of Ran GTPase showed <4 Å fluctuation and noted some acceptable deviation from 41 Å to 44

Å then stayed at equilibrium till the end. RMSD value for ligand fit protein displayed insignificant deviation but after 75ns attained stable equilibrium (4 Å) **(Figure 2, a)**. The RMSF study of selected compound PCPTC provided further proof in favour of RMSD value. The RMSF plot shows the fluctuation of the protein backbone atoms in a molecular dynamic (MD) simulation that provides information about the stability and flexibility of the protein structures, as well as the binding behaviour of ligands or small molecules. The RMSF value of protein showed < 4.5 Å **(Figure 2, b)** and ligand RMSF exhibited < 3.5 Å **(Figure 2, c)**. The stability of the compound was confirmed through extensive testing, making it an ideal candidate for various wet lab experiments.

3.5 Protein-ligand interaction mapping

To map the protein-ligand interaction **(Supplementary Figure 2, a)** for further analysis the docked complex Ran GTPase PCPTC that includes the formation of hydrogen bonds, hydrophobic interactions, ionic interactions and water bridges were extracted from 100ns molecular dynamics (MD) trajectories. Lys^{28} and Lys^{38} both displayed H-bonds where, Lys^{28} showed more than 20% and Lys^{38} displayed 99% H-bonds formation. Val^{40} residue showed both 50% water bridges and 50% hydrophobic interaction. Likewise, for water bridges Thr^{24} and Thr^{25} both residues participated more than 40% of the simulation time. Also, Glu^{36} participated in H-bonds and water-bridges **(Supplementary Figure 2, a)**. This result was further supported by protein-ligand contact **(Supplementary Figure 2, b)**.

3.6 Physical Characterisation of NP

The average size of the PLGA- PCPTC-NP, PGA-PEG-5%-PCPTC-NP and PLGA-PEG-10%- PCPTC-NP was found to be 257.5 nm, 215.2 nm and 166.3 nm, respectively (Table 3). The surface charge for PLGA-PCPTC NP, PLGA-PEG-5%-PCPTC NP and PLGA-PEG-10%-PCPTC NP was found to be -3.2 mV, -1.2 mV and -0.2 mV respectively. The amount of PCPTC encapsulated within the NP was determined and the EE for PLGA-PCPTC NP, PLGA-PEG-5%-PCPTC NP and PLGA-PEG-10%-PCPTC NP was found to be 62.4 %, 71.2 % and 69.5 % respectively.

The three nanoparticles PLGA-PCPTC NP, PLGA-PEG-5%-PCPTC NP and PLGA-PEG-10%-PCPTC NP varied in their average size. The PLGA-PCPTC NP is comparatively bigger with a size measuring 257 nm, and the size of the PLGA-PEG-5%-PCPTC NP and PLGA-

PEG-10%-PCPTC- NP measures 221 nm and 166 nm respectively. The surface charge obtained also varied among the particles. -3.2 mV, for PLGA-PCPTC NP, followed by -1.2 mV for PLGA-PEG-5%-PCPTC NP and -0.2 mV for PLGA-PEG-10%-PCPTC NP. The EE obtained after the determination of the amount of PCPTC encapsulation with NP was found to be 62.4% for PLGA-PCPTC NP, 71.2% for PLGA-PEG-5%-PCPTC NP and 69.5% for PLGA-PEG-10%-PCPTC NP. In this case, PLGA-PEG-5%-PCPTC NP shows a higher amount of EE.

3.7 Morphology- Scanning Electron Microscopy

PCPTC-NP were visualised using SEM to study their morphology. SEM studies showed that the PCPTC-NP were spherical and polydisperse in nature as shown in **Figure 3**.

3.8 Payload Release Study

The release profile of PCPTC-NP was studied for up to 96 hours as shown in **Figure 4**. The formulations used here were PLGA-PCPTC-NP, PLGA-PEG-5%-PCPCTC-NP and PLGA-PEG-10%-PCPCTC-NP. The release pattern, as documented in recent studies, was biphasic **(Figure 4)**. The release of PCPCT seems like a smooth release after the first 12-24 hours followed by the slow and sustained release of PCPTC payload.

This type of release may have happened due to the entrapped drug on the surface of the nanoparticles (Fredenberg et al., 2011). Nearly 50 % of the payload was released after 24 hours in the case of PLGA-PCPTC NP whereas the release was comparatively less in the case of PLGA-PEG-5%-PCPCTC-NP and PLGA-PEG-10%-PCPCTC-NP. Thereafter, the release of the payload was maximum for PLGA-PCPTC NP after 96 hours. It was found to be nearly 60 %. It was found to be 61% and 59 % in the case of PLGA-PEG-5%-PCPCTC-NP and PLGA-PEG-10%-PCPCTC-NP respectively.

3.9 Cellular Uptake- Fluorescence Microscopy

The NP needs to diffuse inside the cells through the plasma membrane to deliver the payload efficiently. An intracellular localisation study of PCPTC-NP in the MDA-MB231 cell line was carried out. NP loaded with coumarin-6 (yellow) and the nucleus was stained with DAPI (blue) **(Figure 5)**. Images were taken using different filters depending on the type of stain of interest. As shown in **Figure 5**, blue patches represent cell's nucleus, yellow represents coumarin 6 dye and the last image was the merged image obtained after merging images of

DAPI with coumarin-6 images obtained from appropriate wavelength channels. It is visible from the image that NP was taken up by the cells successfully. Nanoparticles were localised inside the cells.

3.10 Cell Viability Studies

Cell viability was assessed for MDA-MB231 where cells were transfected using 2.5 μg ml^{-1} (or C1) and 5 μg ml^{-1} (or C2) PCPTC (inside the NP) concentrations. The viability was assessed after 24 hours, 48 hours, 72 hours and 96 hours using MTT. PLGA-PCPTC NP, PLGA-PEG-5%-PCPTC NP and PLGA-PEG-10%-PCPTC NP were used (Table 4). For PLGA-PCPTC NP after 24 hours of treatment cell viability reduced to 78.5 % and 88.2 % for C1 and C2 respectively. Cell viability reduced to half of the original cell population after 72 hours and 96 hours. Whereas blank NP and non-encapsulated drug alone had no significant impact on viability of the cells which confirms that the blank nanoparticles are non-toxic to the cells and the drug is not effective enough when used in its unencapsulated form. PLGA-PEG-5%-PCPTC NP seemed to have an effective effect on cell viability reduction. Cell viability dropped down to 52.3 % after 24 hours and kept on reducing almost proportionally up until 96 hours. The maximum reduction in cell viability observed was 78.7 % at 72 hours where the remaining surviving cell population was found to be 26 % and 21 % for C1 and C2 respectively. A similar reduction in cell viability was also observed with PLGA-PEG-10%-PCPTC NP where cell viability was significantly reduced to 66.5 % after 96 hours.

3.11 Migration Studies- Wound Scratch Assay

The MDA-MB231 cells were treated with Blank NP, unencapsulated PCPTC, PLGA-PCPTC NP, PLGA-PEG-5%-PCPTC NP and PLGA-PEG-10%-PCPTC NP **(Figure 6)**. The treatment was given for 24 hours and 48 hours. The concentration of the payload used was 2.5 μg ml^{-1}. The scratch closure distance affected by payload-loaded NP and unencapsulated PCPTC was measured against the blank NP and untreated cells, respectively. After 24 hours of treatment, 70 % of the MDA-MB231 cells were migrated towards the closure of the scratch in the case of PLGA-PCPTC NP whereas in the case of PLGA-PEG-5%-PCPTC and PLGA-PEG-10 %-PCPTC it was found to be 61 % and 68 % respectively. This rate of migration was reduced further after 48 hours where the distance was covered by the migration of MDA-MB231 cancer cells. 50 %, 45 % and 53 % scratch were closed in the

case of PLGA-PCPTC NP, PLGA-PEG-5%-PCPTC NP and PLGA-PEG-10%-PCPTC NP, respectively.

3.12 Invasion Studies- Transwell membrane Assay

Referring to the result from the MTT assay and Migration assay, PLGA-PEG-5%- PCPTC formulation seemed to be the most effective formulation. Therefore, with this in mind, a cell invasion assay was done where cells were treated with PCPTC, PLGA-PEG-5%-Blank NP and PLGA-PEG-5%-PCPTC NP. 2.5 µg ml^{-1} concentration of PCPTC was used to transfect the cells. The cell invasion was studied on MDA-MB231. When PCPTC-loaded NP was delivered to MDA-MB231, 80 % of the cells were invaded through the membrane after 24 hours whereas invasion was reduced to 63 % after 48 hours **(Figure 7)**. In contrast, there was no effect of blank NP and unencapsulated PCPTC on the cell invasion. This confirms the ineffective nature of the payload when used in unencapsulated form and the non-toxic nature of the NP.

3.13 Ran Pull down Assay

The protein of interest here was Ran-GTPase, therefore, Ran pull-down assay was performed. Ran-GTPase is involved in the functioning of the Ran cycle [8]. Ran pull-down assay results confirmed the decrease in the expression of Ran GTPase on the introduction of PLGA-PEG-5%-PCPTC NP to MDA-MB231 cells. The faint protein band can be seen in lane 3 in **Figure 8**, lane 2 and lane 1 are the bands of control and protein ladder respectively. The size of Ran-GTP was approximately 25 kDa. Active Ran GTP expression was reduced when compared to the untreated cells.

4. Discussion

The primary objective of this research was to identify PCPTC as a potential drug compound that displays an anti-metastatic property by exhibiting high binding affinities with upregulated Ran GTPase in MDA-MB231 breast cancer cells. The interaction between PCPTC and Ran GTPase was studied using molecular docking where we observed favourable binding orientation and intermolecular interactions with the amino acid residues. To further evaluate the binding of the chosen anticancer compound PCPTC, we conducted a molecular dynamics (MD) simulation [20]**.** Integrating the results derived from in silico studies leads us

to postulate that PCPTC may possess inhibitory properties against Ran GTPase and can further be confirmed through biological studies.

The loaded-NP was found to be of different sizes depending on the concentration of PEG associated with the PLGA-PEG complex. The addition of PEG with PLGA in the polymeric formulation reduced the average size of the NP. In addition of PEG, the polymeric length of PLGA moiety reduced which eventually reduced the size of the NP [21]. This may be the reason for the decrease in the size of NP on increasing the amount of PEG in the polymeric formulation.

The value for zeta potential was found to be slightly negative and the extent of negative charge reduced on increasing the PEG concentration in the polymeric formulation. Here, the PLGA used in the study was capped PLGA, i.e., the end carboxylic group in PLGA polymer was masked [7], [22]. This masked the overall surface charge of the NP and eventually reduced the charge [7].

In addition, PEG further masks the overall charge causing a further decrease in the overall negative charge of the formulation. Similarly, Mura et al. 2011 documented a surface charge of -5 mV for PLGA NP which is very close to the range of surface charge values measured in the case of PCPTC NP [23]. Hassan et al. (2015) reported the value of zeta potential was -18.1 mV and Lamichhane et al. (2015) reported -8 mV for PLGA NP which was due to the uncapped functional group present at the end of PLGA polymer [24], [25].

The EE for payload-loaded PLGA-PEG NP was more than PLGA NP. Lapalco et al. (2015) utilised both PLGA and PLGA-PEG polymers to fabricate oxcarbazepine loaded-NP and documented that the addition of PEG to the PLGA polymer increased the encapsulation efficiency. The EE for PLGA and PLGA-PEG NP documented by Lapalco and his colleagues was around 69 % and 72 % respectively [26]. The amount of drug encapsulated inside the NP is a vital dependable variable in drug delivery to minimise the loss of the drug during NP formulation [27].

The release of PCPCT from the NP was biphasic, i.e. primarily smooth release after the first 6 hours followed by the slow and sustained release of PCPTC. This may have happened due to the entrapped drug on the surface of the nanoparticles [28]. 50 % of the payload was released after 24 hours in the case of PLGA-PCPTC NP whereas the release was comparatively less in the case of PLGA-PEG-5%-PCPCTC NP and PLGA-PEG-10%-PCPCTC NP. Thereafter, the release of the payload was maximum for PLGA-PCPTC NP after 96 hours. Drug release from PLGA-based NP can most commonly be either biphasic or

triphasic and rarely monophasic [29]. The entire release of payload from the NP in a sustained manner is extremely important to keep the payload concentration constant inside the cellular environment. Koopaei et al (2014) fabricated PLGA-PEG NP to encapsulate doxotaxel and payload release studies confirmed the biphasic release pattern [30]. Drug release from PLGA-based NP can most commonly be either biphasic or triphasic and rarely monophasic.

The nanoparticles need to diffuse inside the cells through the plasma membrane to deliver the payload efficiently. An intracellular localisation study of PCPTC-NP in the MDA-MB231 cell line was carried out. It is visible from the image **(Figure 5)** that NP wastaken up by the cells successfully. Nanoparticles were localised inside the cells. It was confirmed from the release studies that PCPTC-NP released the drug efficiently and the intracellular uptake study shows that the NP were taken up by the cell. Therefore, it would be fair to conclude that the PCPTC-loaded NP were endocytosed by the cells and released the payload.

For PLGA-PCPTC NP (Table 2), after 24 hours of treatment cell viability reduced significantly to 78 % (*P<0.05) and 88 % (*P<0.05) for C1 and C2 respectively. Cell viability reduced to half of the original cell population after 72 hours and 96 hours. Whereas blank NP and non-encapsulated drug alone had no significant impact on the viability of the cells which confirms that the blank nanoparticles were non-toxic to the cells and the unencapsulated drug was not found to be cell permeable of its own, hence did not exhibit any impact on cell viability. On the other hand, PLGA-PEG-5%-PCPTC NP significantly reduced cell viability to 50 % (***P< 0.001) after 24 hours due to the burst release of the payload and kept on reducing proportionally until 96 hours due to the sustained release of the payload. The maximum reduction in cell viability was observed at 72 hours where the remaining surviving cell population was found to be 26 % and 21 % for C1 and C2 respectively (***P<0.001). Similar but comparatively less effective cell viability reductions were seen in the case of PLGA-PEG-10%-PCPTC NP where cell viability was reduced to 39 % (C1) and 44 % (C2) after 24 hours (***P<0.001) and remained low till 96 due to the sustained release of PCPCT from NP. In all the polymeric formulations, there was no significant toxicity observed in the case of blank NP and non-encapsulated drugs.

Cellular toxicity is one of the most important parameters in drug delivery. Various anti-cancerous agents such as paclitaxel, trifluoperazine and doxorubicin have been used to assess their toxicity in cancer cells [31], [32]. Successful reduction in cancer cell viability using such anti-cancer agents has also been reported [33]. Choi et al 2020 reported a significant reduction in CT-26 tumour cell viability when the cells were treated with doxorubicin PLGA-

NP for 48 hours similar to what was observed in the case of PLGA PEG 5% PCPTC NP. The cell viability of doxorubicin-PLGA NP treated CT-26 tumour cells is reduced at various doxorubicin concentrations ranging from 0.001μM to 10μM. The cell viability rate at 0.001μM doxorubicin concentration shows around 100% reduction, which gradually decreases to less than 20% at 10μM concentration in CT-26 tumour cells when using doxorubicin PLGA-NP [33].

Migration of cancer cells is one of the root causes of the high mortality rate in cancer patients which needs to be addressed. Migration is one of the important characteristics of cancer cells. Here, PCPTC NP (PLGA-PCPTC NP and PLGA-PEG-PCPTC NP) significantly reduced the migration of the cells after 24/48 hours (***P<0.001). A similar reduction was observed in the migration of HCC liver carcinoma cells by inhibiting the activity of aldehyde dehydrogenase on the introduction of disulfiram-loaded PLGA NP [34]. Also, a significant reduction in MDA-MB231 cell migration was reported due to the blocking of the NFκβ signalling pathway when cells were transfected by celastrol-loaded NP [27], [35]. Here, PCPTC blocked the ran cycle which eventually inhibited migration of the cells by interrupting the cell cycle which was confirmed later on by performing a Ran Pull down assay.

The highly invasive nature of the cancer cells is another problem which needs to be resolved to improve treatment against cancer PCPTC-loaded NP delivered to MDA-MB231, 80 % of the cells were invaded through the membrane after 24 hours whereas invasion reduced to 63 % after 48 hours **(Figure 7)**. This explains the high potency of PCPTC against highly invasive breast cancer cells. The reduction in cellular invasion after 48 hours was due to the steady and sustained release of PCPTC from NP. In contrast, there was no effect of blank NP and unencapsulated PCPTC on the cell invasion. This confirms the ineffective nature of the payload when used in unencapsulated form and the non-toxic nature of the NP.

Various drug-carrying vehicles have been utilised to deliver anti-invasive cancer drugs for cancer therapeutics which significantly inhibited cancer cell invasion. Zou et al., 2020 developed quercetin-loaded NP to study TNBC invasion and inhibitory effect in 4T1 and MDA-MB231 cell lines. When compared to the 0μM quercetin control group, incubating 4T1 cells with 10μM of free quercetin resulted in a 77.5 % reduction in cell invasion rate and a 9.8 % reduction in cell invasion rate with Qu-NP [30]. In the MDA-MB231 cell line 42% cell invasion reduction when treated with 10μM free quercetin and an 18.1% reduction rate in Qu-NP, finalising Qu-NP has a better inhibitory effect than free quercetin [36].

The protein of interest here was Ran-GTPase, therefore, Ran pull-down assay was performed. Ran-GTPase is involved in the functioning of the Ran cycle [10]. Ran cycle is responsible for the transportation of molecules from the nucleus to the cytoplasm and vice-versa [37]. It is also responsible for spindle formation and cell cycle progression during mitosis [38]. We aimed to inhibit the conversion of inactive Ran-GDP into Ran-GTP to block the Ran cycle, which will inhibit metastasis in cancer cells [39]. Results obtained after performing a Ran pull down assay suggested that PCPCT successfully reduced the expression of Ran-GTPase in Ran cycle in MDA-MB231 cells. The bands of the sample treatment appeared to be significantly fainted as compared to the control where no treatment was given. Active Ran GTPase expression was reduced greatly when compared to the untreated cells which confirmed the ability of PCPTC to block the ran cycle and hence caused anti-metastatic effects.

5. Conclusion

The ability of nanoparticles to deliver payload to the target site is a promising approach in cancer therapeutics. In this study, PCPTC was selected based on a strong docking score >-7 kcal/mol with Ran GTPase. The respective complex was further evaluated in terms of intermolecular interaction, complex stability and binding affinity against Ran GTPase using computational methods. Based on the collective analysis, the selected compound PCPTC was concluded with strong molecular contacts in the active pocket of Ran GTPase. Hence, the compound can be considered for further evaluation as a Ran GTPase inhibitor using in vitro studies for drug development against breast cancer.

Here, PCPTC-loaded nanoparticulate formulations were developed to deliver the payload to breast cancer cells. PCPTC-NP were small spherical bodies and showed significant encapsulation efficiency. The release of the payload from nanoparticles was found to be biphasic. PCPTC-NP, on delivery to breast cancer cells, showed a significant decrease in cell viability. Also, the migration studies and invasion studies confirmed that the migration and invasion of the cancer cells were significantly inhibited by the PCPTC-NP. PCPTC-NP. From the results obtained from cell viability studies and migration studies, PLGA-PEG-5%-PCPTC NP was found to be most effective and carried further for the rest of the *in vitro* studies, such as the invasion study and Ran pull-down assay. The reduction of Ran-GTPase was confirmed

by Ran pull-down assay where PCPTC-loaded NP successfully inhibited the production of Ran-GTPase, and hence stopping metastasis in cancer cells.

Table 1

Docking energy of PCPTC against Ran GTPase

Compound	Binding Energy (kcal/mol)	Re-docked Energy (kcal/mol)
RanGTPase-PCPTC(N-3-[pyridine-4-yl)carbamoyl] phenyl] thiophene-2-carboxamide)	-7.4	-7.4

Table 2

Intramolecular interaction analysis of Ran GTPase with PCPTC

Complex	**Hydrophobic**	**Polar**	**II-II stacking/II-II Cation**	**Positive**	**Negative**	**II cation**	**Glycine**
Ran GTPase PCPTC	Ala^{151},Ile^{126}, Val^{40},Tyr^{39}, Phe^{35}	Ser^{150}, Asn^{122}, Thr^{25},Thr^{24}, Thr^{21}	Tyr^{39}, Phe^{35}	Lys^{152}, Lys^{123}, Lys^{38}, Lys^{23}	Asp^{125}	Lys^{152}	Gly^{20}, Gly^{22}

Table 3

Physical characterisation of PCPTC-loaded nanoparticles where size, polydispersity index (PDI), zeta potential and encapsulation efficiency (EE) of the loaded NP were determined (n = 6)

	Size (nm)	**PDI**	**Zeta Potential (mV)**	**Encapsulation efficiency (%)**
PLGA-PCPTC NP	257.5±12.1	0.221±0.01	-3.2±0.4	62.4±3.7
PLGA-PEG-5%-PCPTC NP	215.2±94.0	0.537±0.10	-1.2±0.6	71.2±0.6
PLGA-PEG-10%-PCPTC NP	166.3±48.6	0.346±0.03	-0.2±0.0	69.5±3.0

Table 4

Cell proliferation (%) study of PCPTC NP on MDA-MB231 breast cancer cell line, values are mean ± SD (n=3). C1 and C2 represent concentrations of PCPTC used to transfect the cells, C1 & C2 refer to 1 µg ml^{-1} & 2.5 µg ml^{-1}, respectively

	24 Hours	48 Hours	72 Hours	96 Hours
Cells	100±8.9	100±9.9	100±2.8	100.3±6.8
PCPTC (2.5 µg)	102±3.4	91.0±9.3	90.8±6.8	92.3±3.6
PLGA-Blank NP	95.7±2.0	96.0±1.7	107.9±0.7	100.0±1.6
PLGA-PEG-5%-Blank NP	110.6±2.9	101.37±2.4	92.5±1.5	101.0±9.6
PLGA-PEG-10%-Blank NP	99.2±5.5	99.18±1.8	103±1.4	99.4±7.3
PLGA-PCPTC -C1 NP	78.5±5.8	50.9±9.6	46.2±6.3	58.9±4.5

PLGA-PCPTC -C2 NP	88.2±8.5	34.8±4.9	41.2±8.2	70.1±6.4
PLGA-PEG-5%-PCPTC -C1 NP	52.3±5.8	51.3±3.7	26.1±10.6	31.5±1.7
PLGA-PEG-5%-PCPTC –C2 NP	47.0±1.8	46.8±4.0	21.3±5.9	31.1±7.8
PLGA-PEG-10%-PCPTC -C1 NP	39.4±5.0	44.5±7.5	56.5±3.2	66.5±2.6
PLGA-PEG-10%-PCPTC –C2 NP	45.9±2.5	41.7±2.9	67.2±2.9	48.8±4.4

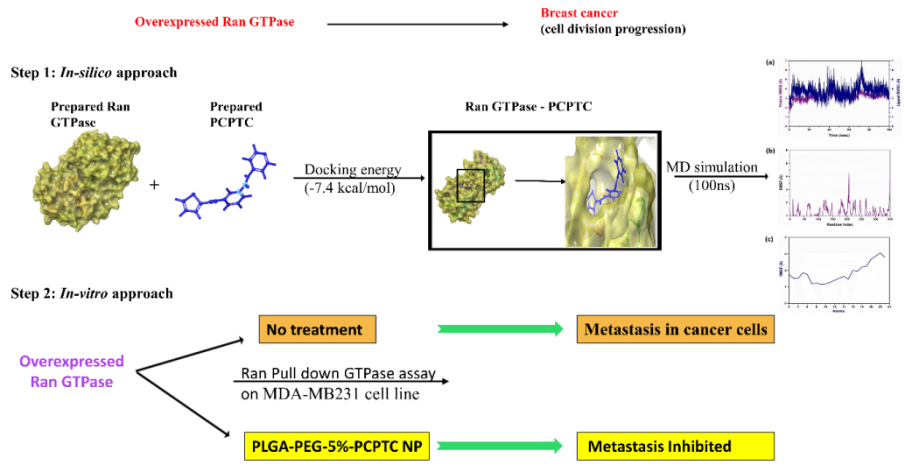

Graphical Abstract: Schematic representation of different steps followed for the discovery of anticancer compound against Ran GTPase

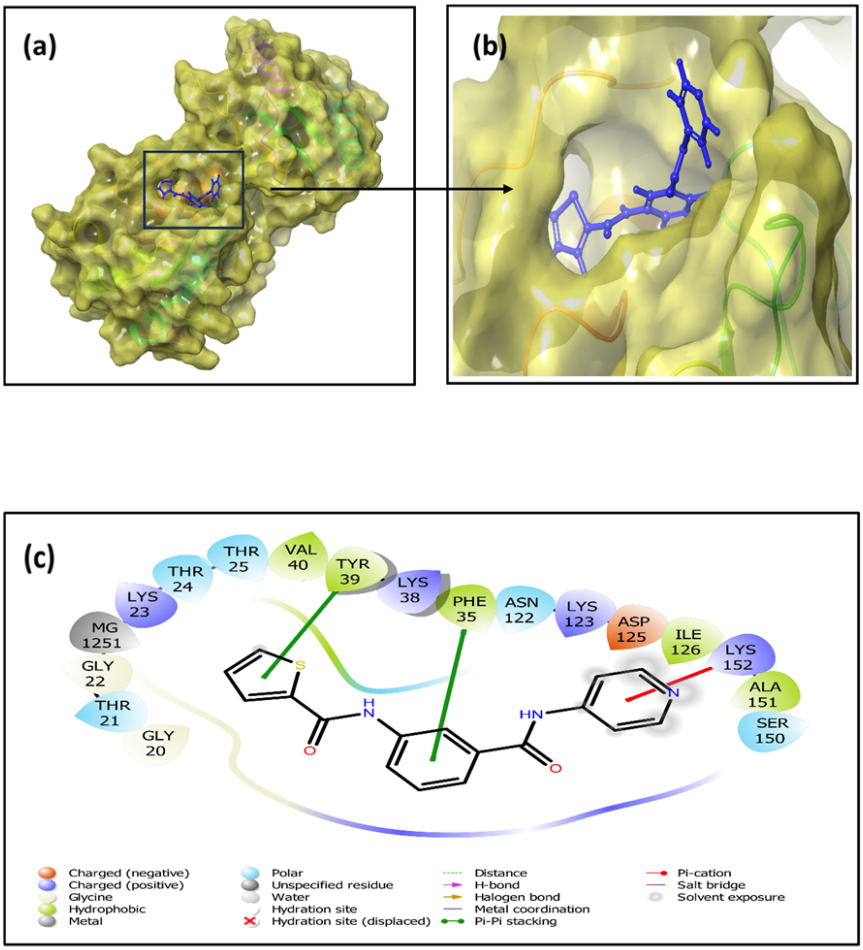

Figure 1

(a) 3D structure of PCPTC against Ran GTPase, (b) full 3D structure of PCPTC against Ran GTPase, (c) 2D interaction of PCPTC with Ran GTPase.

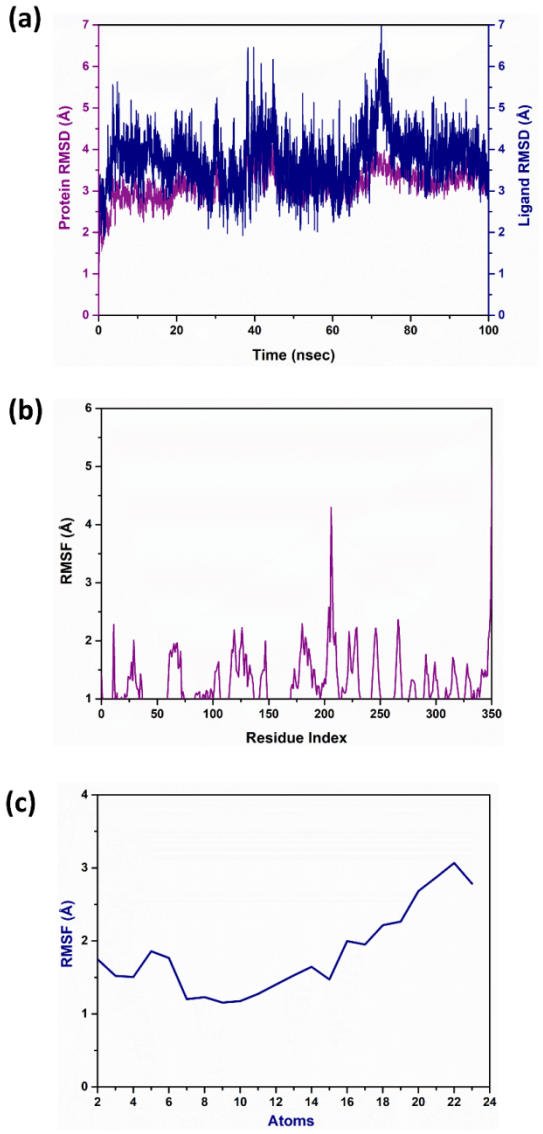

Figure 2

(a) RMSD values for the alpha carbon atoms of the Ran GTPase are shown as purple curves, and ligand PCPTC are shown as blue curves of the docked complexes.

(b) RMSF plot of WDR5-MYC with PCPTC.

(c) RMSF plot of selected ligand PCPTC.

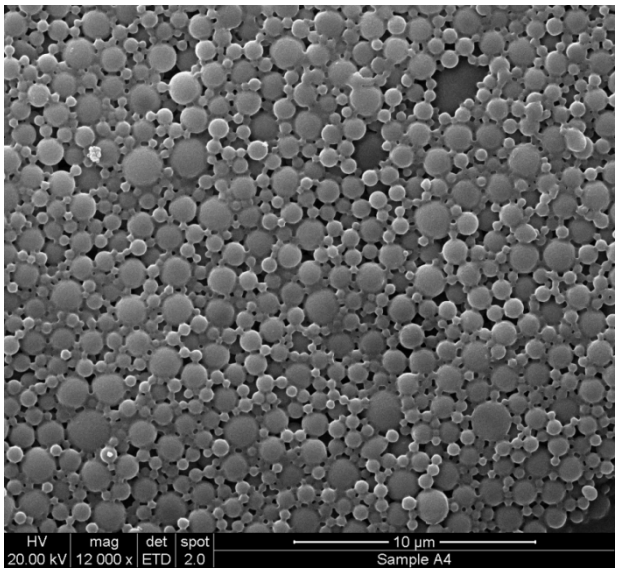

Figure 3

Scanning electron microscopic image of PCPTC loaded NP where parameters used were magnification 12 000×, voltage was 20.0 kV.

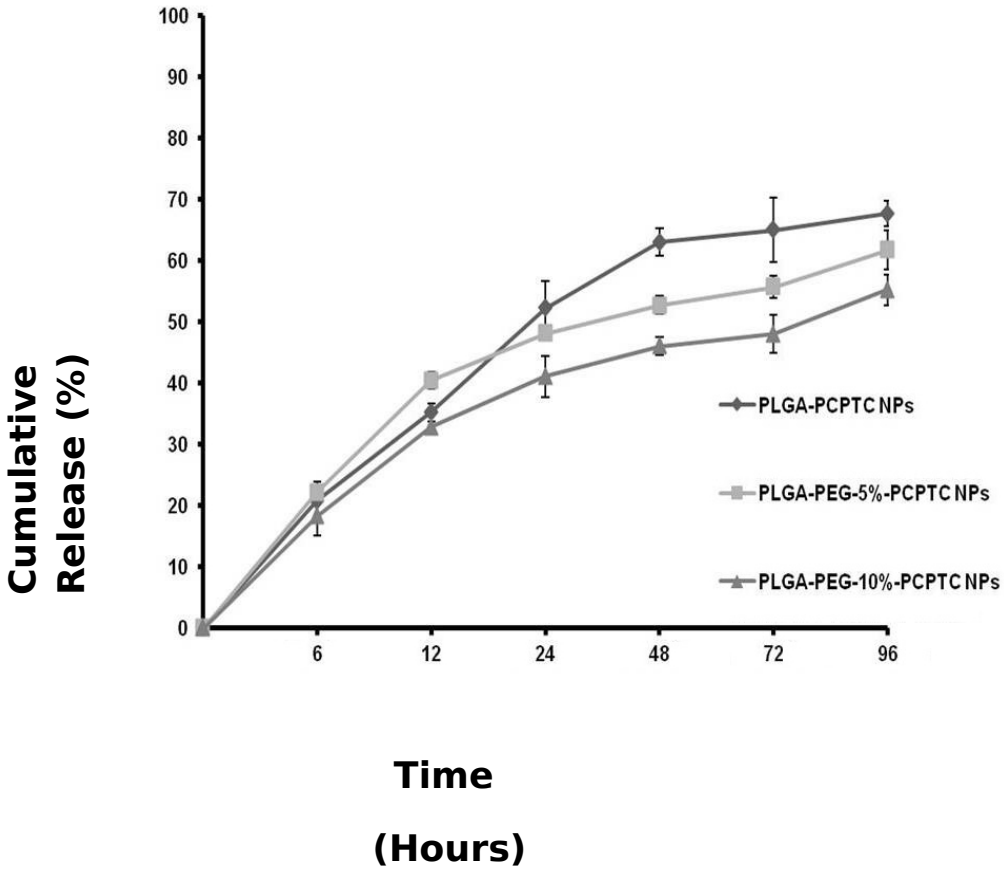

Figure 4

Cumulative release profile of PCPTC-loaded nanoparticles where percentage of payload released was determined on following time intervals (0h, 6h, 12h, 24h, 48h, 72h and 96h, h = hours), (n=3).

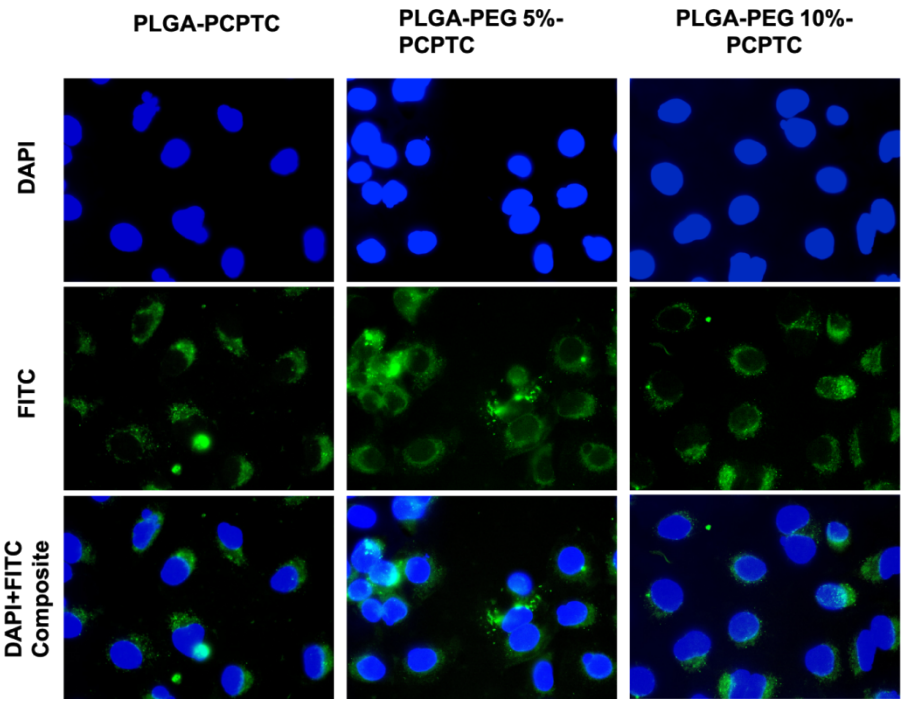

Figure 5

Intracellular localisation of PCPTC-loaded nanoparticles in MDA-MB231 cancer cell line where two channels were used to capture images, i.e., DAPI channel (λ_{ex}-358nm, λ_{em}-461 nm) for visualising blue stained nucleus and FITC (λ_{ex}-488 nm, λ_{em}-519 nm) for visualizing Coumarin-6 loaded- PCPTC-loaded PLGA & PEGylated PLGA NP.

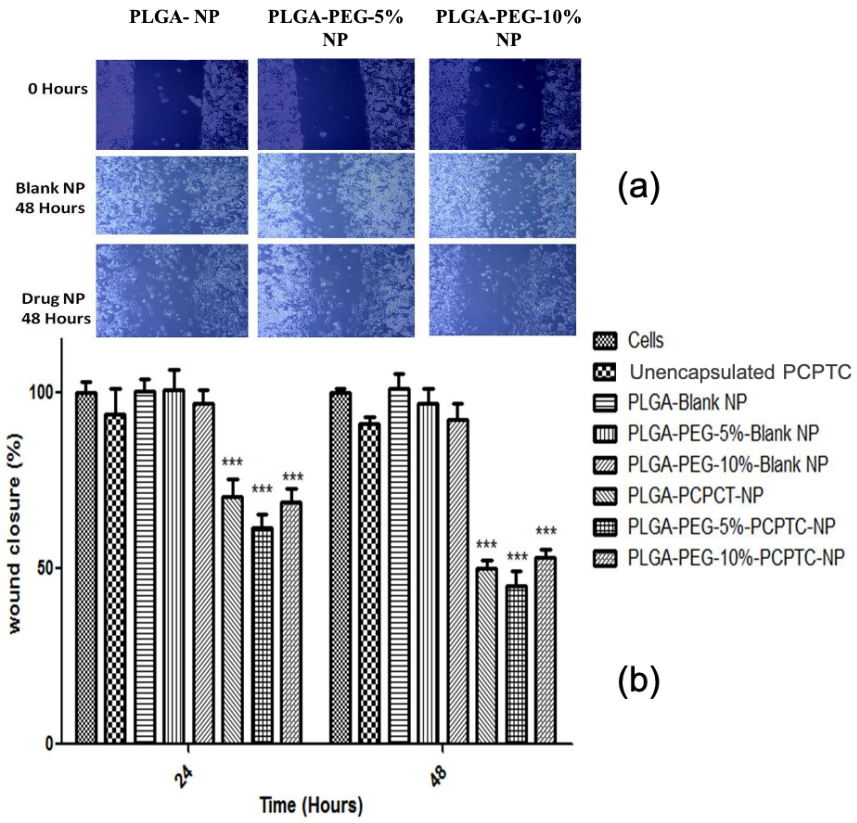

Figure 6

Scratch assay on MDA-MB231 Cell line, (A) microscopic images of effect of PCPTC-loaded NP on cell migration, (B) graphical representation of effect of PCPTC-loaded NP on the rate of migration of MDA-MB231 cells up to 48 hours. PCPTC Concentration used was 2.5 µg ml^{-1}. Values are mean ± SD with n=3. *P<0.05, **P<0.01, ***P<0.001,

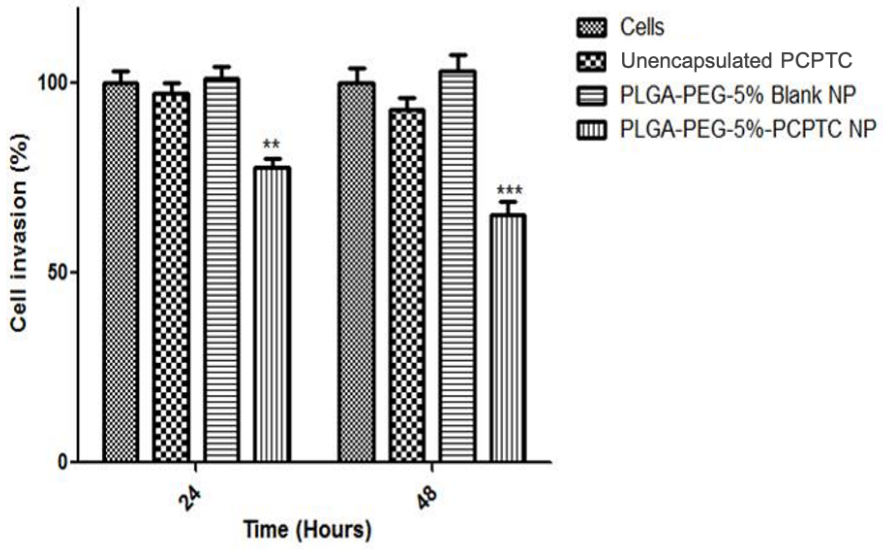

Figure 7

Invasion studies showing the effect of PLGA-PEG-5%-PCPTC NP on invasion of MDA-MB231 cells. Values are mean ± SD with n=3. *P<0.05, **P<0.01, ***P<0.001, where cell invasion reduced by loaded-NP were compared with the cell invasion obtained by blank-NP

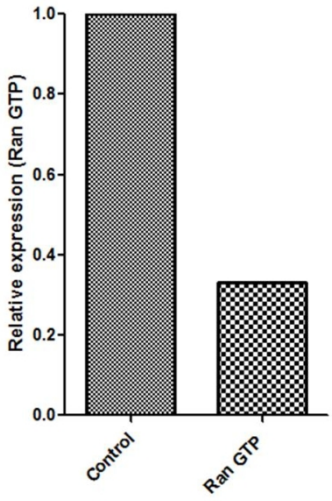

Figure 8

Ran Pull-Down assay result of Ran GTPase in MDA-MB231 cells, Where, Lane 1 is control (supernatant of the cells without treatment), Lane 2 is PLGA-PEG-5%-PCPTC-NP (supernatant of the cells treated with PLGA-PEG-5%-PCPTC NP). The bar graph shows the quantitative reduction of the percentage of active Ran GTP on introduction of PCPTC-NP, the expression of Ran GTP in treated cells were found to be 33.2 % relative to the untreated cells.

Declarations

Ethics approval Not applicable

Consent to participate This research does not contain any studies with human participants performed by any of the authors.

Consent to publish free

Author contribution Ankur Sharma: Conceptualization writing and editing the original draft and revising, writing and editing the discussion. Amka Nagar: Writing and editing the *in-silico* part, revising and discussing the results and writing the discussion. Susan Hawthorne: Evaluating, revising and editing the discussion. Mohini Singh: She evaluated the data and provided critical feedback. All authors have read and accepted the final version of the manuscript.

Funding This research received no external funding.

Competing interests The authors declare no conflict of interest.

Availability of data and materials All experimental data and analyses of the study are included in this manuscript.

Acknowledgement: We thanks Prof. Ana Claudia Santos (University of Coimbra, Portugal) for her support.

References

[1] R. L. Anderson *et al.*, "A framework for the development of effective anti-metastatic agents," *Nat Rev Clin Oncol*, vol. 16, no. 3, pp. 185–204, Mar. 2019, doi: 10.1038/s41571-018-0134-8.

[2] Ketabat *et al.*, "Controlled Drug Delivery Systems for Oral Cancer Treatment—Current Status and Future Perspectives," *Pharmaceutics*, vol. 11, no. 7, p. 302, Jun. 2019, doi: 10.3390/pharmaceutics11070302.

[3] H. S. Tuli *et al.*, "Molecular Mechanisms of Action of Genistein in Cancer: Recent Advances," *Front. Pharmacol.*, vol. 10, p. 1336, Dec. 2019, doi: 10.3389/fphar.2019.01336.

[4] V. Mishra, P. Nayak, N. Yadav, M. Singh, M. M. Tambuwala, and A. A. A. Aljabali, "Orally administered self-emulsifying drug delivery system in disease management: advancement and patents," *Expert Opinion on Drug Delivery*, vol. 18, no. 3, pp. 315–332, Mar. 2021, doi: 10.1080/17425247.2021.1856073.

[5] Y. Dang and J. Guan, "Nanoparticle-based drug delivery systems for cancer therapy," *Smart Materials in Medicine*, vol. 1, pp. 10–19, 2020, doi: 10.1016/j.smaim.2020.04.001.

[6] R. Kaur and P. Khullar, "Research Progress to Improve Solubility and Drug-Releasing Curcumin Properties with Nanoencapsulation," *Chemical Nanoscience and Nanotechnology: New Materials and Modern Techniques*, p. 241, 2019.

[7] A. Sharma *et al.*, "Effects of curcumin-loaded poly(lactic-co-glycolic acid) nanoparticles in MDA-MB231 human breast cancer cells," *Nanomedicine*, vol. 16, no. 20, pp. 1763–1773, Aug. 2021, doi: 10.2217/nnm-2021-0066.

[8] Y.-R. Liao *et al.*, "The novel carboxamide analog ITR-284 induces caspase-dependent apoptotic cell death in human hepatocellular and colorectal cancer cells," *Molecular Medicine Reports*, vol. 7, no. 5, pp. 1539–1544, May 2013, doi: 10.3892/mmr.2013.1359.

[9] J.-S. Yang, C.-A. Lin, C.-C. Lu, Y.-F. Wen, F.-J. Tsai, and S.-C. Tsai, "Carboxamide analog ITR-284 evokes apoptosis and inhibits migration ability in human lung

adenocarcinoma A549 cells," *Oncology Reports*, vol. 37, no. 3, pp. 1786–1792, Mar. 2017, doi: 10.3892/or.2017.5374.

[10] Z. Boudhraa, E. Carmona, D. Provencher, and A.-M. Mes-Masson, "Ran GTPase: A Key Player in Tumor Progression and Metastasis," *Front. Cell Dev. Biol.*, vol. 8, p. 345, May 2020, doi: 10.3389/fcell.2020.00345.

[11] Y. A. Haggag *et al.*, "Nano-encapsulation of a novel anti-Ran-GTPase peptide for blockade of regulator of chromosome condensation 1 (RCC1) function in MDA-MB-231 breast cancer cells," *International Journal of Pharmaceutics*, vol. 521, no. 1–2, pp. 40–53, Apr. 2017, doi: 10.1016/j.ijpharm.2017.02.006.

[12] M. S. Zhang, M. Furuta, A. Arnaoutov, and M. Dasso, "RCC1 regulates inner centromeric composition in a Ran-independent fashion," *Cell Cycle*, vol. 17, no. 6, pp. 739–748, Mar. 2018, doi: 10.1080/15384101.2018.1442630.

[13] L. Qiao *et al.*, "Regulator of chromatin condensation 1 abrogates the G1 cell cycle checkpoint via Cdk1 in human papillomavirus E7-expressing epithelium and cervical cancer cells," *Cell Death Dis*, vol. 9, no. 6, p. 583, May 2018, doi: 10.1038/s41419-018-0584-z.

[14] J. Zhou *et al.*, "GEF-independent Ran activation shifts a fraction of the protein to the cytoplasm and promotes cell proliferation," *Mol Biomed*, vol. 1, no. 1, p. 18, Dec. 2020, doi: 10.1186/s43556-020-00011-2.

[15] E. F. Pettersen *et al.*, "UCSF Chimera?A visualization system for exploratory research and analysis," *J. Comput. Chem.*, vol. 25, no. 13, pp. 1605–1612, Oct. 2004, doi: 10.1002/jcc.20084.

[16] T. Sander, "OSIRIS property explorer," *Organic Chemistry Portal*, pp. 1099–0690,

[17] A. Daina, O. Michielin, and V. Zoete, "SwissADME: a free web tool to evaluate pharmacokinetics, drug-likeness and medicinal chemistry friendliness of small molecules," *Sci Rep*, vol. 7, no. 1, p. 42717, Mar. 2017, doi: 10.1038/srep42717.

[18] "Desmond Molecular Dynamics System, D. E. Shaw Research, New York, NY, 2020-4. Maestro-Desmond Interoperability Tools, Schrödinger, New York, NY, 2020-4.".

[19] M. Chouhan *et al.*, "Inhibition of *Mycobacterium tuberculosis* resuscitation-promoting factor B (RpfB) by microbially derived natural compounds: a computational study," *Journal of Biomolecular Structure and Dynamics*, pp. 1–12, May 2023, doi: 10.1080/07391102.2023.2208214.

[20] T. Mahaddalkar, C. Suri, P. K. Naik, and M. Lopus, "Biochemical characterization and molecular dynamic simulation of β-sitosterol as a tubulin-binding anticancer agent," *European Journal of Pharmacology*, vol. 760, pp. 154–162, Aug. 2015, doi: 10.1016/j.ejphar.2015.04.014.

[21] A. Sharma, P. McCarron, K. Matchett, S. Hawthorne, and M. El-Tanani, "Anti-Invasive and Anti-Proliferative Effects of shRNA-Loaded Poly(Lactide-Co-Glycolide) Nanoparticles Following RAN Silencing in MDA-MB231 Breast Cancer Cells," *Pharm Res*, vol. 36, no. 2, p. 26, Feb. 2019, doi: 10.1007/s11095-018-2555-6.

[22] L. Zhou *et al.*, "Codelivery of SH-aspirin and curcumin by mPEG-PLGA nanoparticles enhanced antitumor activity by inducing mitochondrial apoptosis," *IJN*, p. 5205, Aug. 2015, doi: 10.2147/IJN.S84326.

[23] E. Fattal *et al.*, "Influence of surface charge on the potential toxicity of PLGA nanoparticles towards Calu-3 cells," *IJN*, p. 2591, Oct. 2011, doi: 10.2147/IJN.S24552.

[24] A. Hassan, K. Hosny, Z. Murshid, A. Alhadlaq, A. Yamani, and G. Naguib, "Depot injectable biodegradable nanoparticles loaded with recombinant human bone morphogenetic protein-2: preparation, characterization, and in vivo evaluation," *DDDT*, p. 3599, Jul. 2015, doi: 10.2147/DDDT.S79812.

[25] P. Shastri, S. Lamichhane, N. Arya, N. Ojha, and E. Kohler, "Glycosaminoglycan-functionalized poly-lactide-co-glycolide nanoparticles: synthesis, characterization, cytocompatibility, and cellular uptake," *IJN*, p. 775, Jan. 2015, doi: 10.2147/IJN.S73508.

[26] E. Rytting, H. Ali, N. Denora, and A. Lopalco, "Oxcarbazepine-loaded polymeric nanoparticles: development and permeability studies across in vitro models of the blood–brain barrier and human placental trophoblast," *IJN*, p. 1985, Mar. 2015, doi: 10.2147/IJN.S77498.

[27] A. Sharma *et al.*, "Nanoparticulate RNA delivery systems in cancer," *Cancer Reports*,

[28] C. Rodrigues De Azevedo *et al.*, "Modeling of the burst release from PLGA micro- and nanoparticles as function of physicochemical parameters and formulation characteristics," *International Journal of Pharmaceutics*, vol. 532, no. 1, pp. 229–240, Oct. 2017, doi: 10.1016/j.ijpharm.2017.08.118.

[29] L. Pourtalebi Jahromi, M. Ghazali, H. Ashrafi, and A. Azadi, "A comparison of models for the analysis of the kinetics of drug release from PLGA-based nanoparticles," *Heliyon*, vol. 6, no. 2, p. e03451, Feb. 2020, doi: 10.1016/j.heliyon.2020.e03451.

[30] M. N. Koopaei *et al.*, "Docetaxel loaded PEG-PLGA nanoparticles: optimized drug loading, in-vitro cytotoxicity and in-vivo antitumor effect," *Iranian journal of pharmaceutical research: IJPR*, vol. 13, no. 3, p. 819, 2014.

[31] A. Pulkoski-Gross *et al.*, "Repurposing the Antipsychotic Trifluoperazine as an Antimetastasis Agent," *Mol Pharmacol*, vol. 87, no. 3, pp. 501–512, Mar. 2015, doi: 10.1124/mol.114.096941.

[32] S. Yang, I.-C. Sun, H. S. Hwang, M. K. Shim, H. Y. Yoon, and K. Kim, "Rediscovery of nanoparticle-based therapeutics: boosting immunogenic cell death for potential application in cancer immunotherapy," *J. Mater. Chem. B*, vol. 9, no. 19, pp. 3983–4001, 2021, doi: 10.1039/D1TB00397F.

[33] Y. Choi *et al.*, "Doxorubicin-Loaded PLGA Nanoparticles for Cancer Therapy: Molecular Weight Effect of PLGA in Doxorubicin Release for Controlling Immunogenic Cell Death," *Pharmaceutics*, vol. 12, no. 12, p. 1165, Nov. 2020, doi: 10.3390/pharmaceutics12121165.

[34] Z. Wang *et al.*, "Poly lactic-co-glycolic acid controlled delivery of disulfiram to target liver cancer stem-like cells," *Nanomedicine: Nanotechnology, Biology and Medicine*, vol. 13, no. 2, pp. 641–657, Feb. 2017, doi: 10.1016/j.nano.2016.08.001.

[35] J. Shi *et al.*, "Celastrol: A Review of Useful Strategies Overcoming its Limitation in Anticancer Application," *Front. Pharmacol.*, vol. 11, p. 558741, Nov. 2020, doi: 10.3389/fphar.2020.558741.

[36] Y. Zhou *et al.*, "Improved therapeutic efficacy of quercetin-loaded polymeric nanoparticles on triple-negative breast cancer by inhibiting uPA," *RSC Adv.*, vol. 10, no. 57, pp. 34517–34526, 2020, doi: 10.1039/D0RA04231E.

[37] Y. Haggag *et al.*, "Co-delivery of a RanGTP inhibitory peptide and doxorubicin using dual-loaded liposomal carriers to combat chemotherapeutic resistance in breast cancer cells," *Expert Opinion on Drug Delivery*, vol. 17, no. 11, pp. 1655–1669, Nov. 2020, doi: 10.1080/17425247.2020.1813714.

[38] Y. Haggag *et al.*, "Novel Ran-RCC1 Inhibitory Peptide-Loaded Nanoparticles Have Anti-Cancer Efficacy In Vitro and In Vivo," *Cancers*, vol. 11, no. 2, p. 222, Feb. 2019, doi: 10.3390/cancers11020222.

[39] C. Sheng *et al.*, "Knockdown of Ran GTPase expression inhibits the proliferation and migration of breast cancer cells," *Molecular medicine reports*, vol. 18, no. 1, pp. 157–168, 2018.

List of Tables

Table 1

Docking energy of PCPTC against Ran GTPase

Complex	**Virtual screening (binding energy with target RanGTPase) Kcal/mol**
RanGTPase-PCPTC(N-3-[pyridine-4-yl)carbamoyl] phenyl] thiophene-2-carboxamide)	-7.4 Kcal/mol

Table 2

Intramolecular interaction analysis of Ran GTPase with PCPTC

Complex	**Hydrophobic**	**Polar**	**II-II stacking/II-II Cation**	**Positive**	**Negative**	**II cation**	**Glycine**
Ran GTPase PCPTC	Ala[151],Ile[126], Val[40],Tyr[39], Phe[35]	Ser[150], Asn[122], Thr[25],Thr[24],	Tyr[39], Phe[35]	Lys[152], Lys[123], Lys[38], Lys[23]	Asp[125]	Lys[152]	Gly[20], Gly[22]

	Thr^{21}

Table 3

Physical characterisation of PCPTC-loaded nanoparticles where size, polydispersity index (PDI), zeta potential and encapsulation efficiency (EE) of the loaded NP were determined (n = 6)

	Size (nm)	**PDI**	**Zeta Potential (mV)**	**Encapsulation efficiency (%)**
PLGA-PCPTC NP	257.5±12.1	0.221±0.01	-3.2±0.4	62.4±3.7
PLGA-PEG-5%-PCPTC NP	215.2±94.0	0.537±0.10	-1.2±0.6	71.2±0.6
PLGA-PEG-10%-PCPTC NP	166.3±48.6	0.346±0.03	-0.2±0.0	69.5±3.0

Table 4

Cell proliferation (%) study of PCPTC NP on MDA-MB231 breast cancer cell line, values are mean ± SD (n=3). C1 and C2 represent concentrations of PCPTC used to transfect the cells, C1 & C2 refer to 1 μg ml^{-1} & 2.5 μg ml^{-1}, respectively

	24 Hours	48 Hours	72 Hours	96 Hours	
Cells	100±8.9	100±9.9	100±2.8	100.3±6.8	
PCPTC (2.5 μg)	102±3.4	91.0±9.3	90.8±6.8	92.3±3.6	+*
PLGA-Blank NP	95.7±2.0	96.0±1.7	107.9±0.7	100.0±1.6	
PLGA-PEG-5%-Blank NP	110.6±2.9	101.37±2.4	92.5±1.5	101.0±9.6	
PLGA-PEG-10%-Blank NP	99.2±5.5	99.18±1.8	103±1.4	99.4±7.3	
PLGA-PCPTC -C1 NP	78.5±5.8	50.9±9.6	46.2±6.3	58.9±4.5	
PLGA-PCPTC -C2 NP	88.2±8.5	34.8±4.9	41.2±8.2	70.1±6.4	
PLGA-PEG-5%-PCPTC -C1 NP	52.3±5.8	51.3±3.7	26.1±10.6	31.5±1.7	
PLGA-PEG-5%-PCPTC –C2 NP	47.0±1.8	46.8±4.0	21.3±5.9	31.1±7.8	
PLGA-PEG-10%-PCPTC -C1 NP	39.4±5.0	44.5±7.5	56.5±3.2	66.5±2.6	
PLGA-PEG-10%-PCPTC –C2 NP	45.9±2.5	41.7±2.9	67.2±2.9	48.8±4.4	

List of Figures

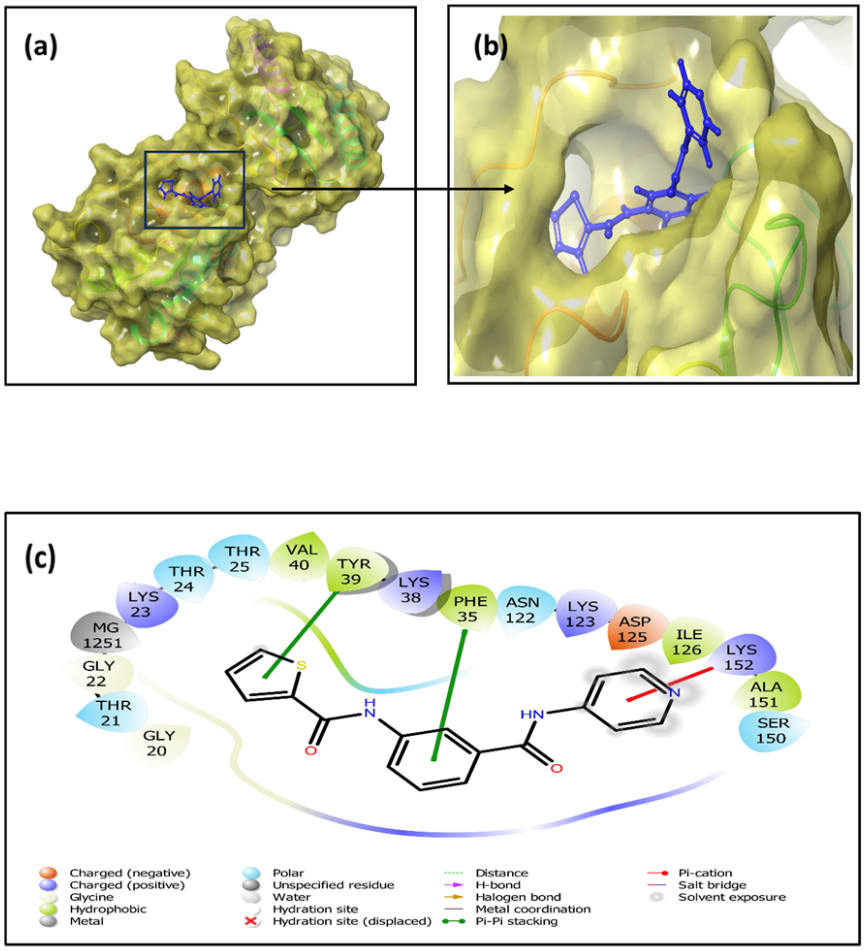

Figure 1

(a) 3D structure of PCPTC against Ran GTPase, (b) full 3D structure of PCPTC against Ran GTPase,

(c) 2D interaction of PCPTC with Ran GTPase.

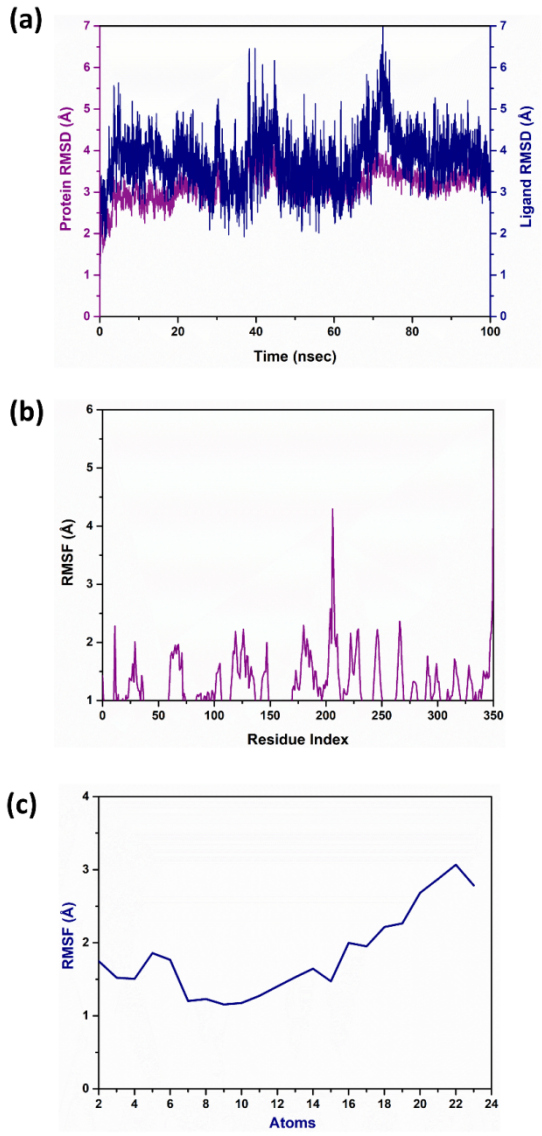

Figure 2

(a) RMSD values for the alpha carbon atoms of the Ran GTPase are shown as purple curves, and ligand PCPTC is shown as blue curves of the docked complexes.

(b) RMSF plot of WDR5-MYC with PCPTC.

(c) RMSF plot of selected ligand PCPTC.

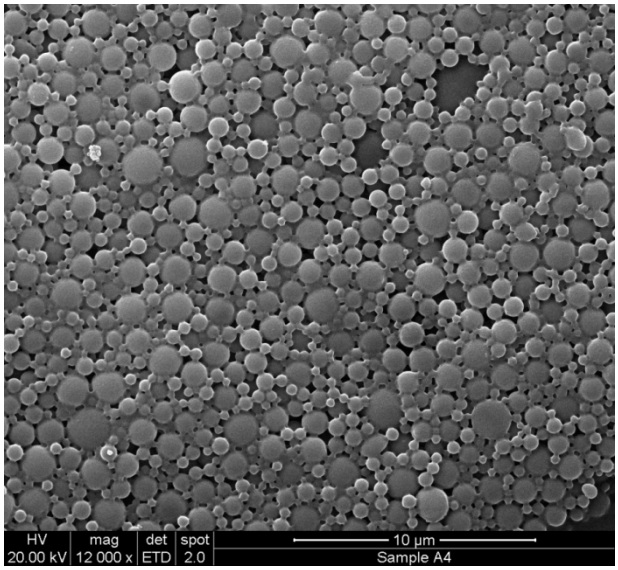

Figure 3

Scanning electron microscopic image of PCPTC loaded NP where parameters used were magnification 12 000×, voltage was 20.0 kV.

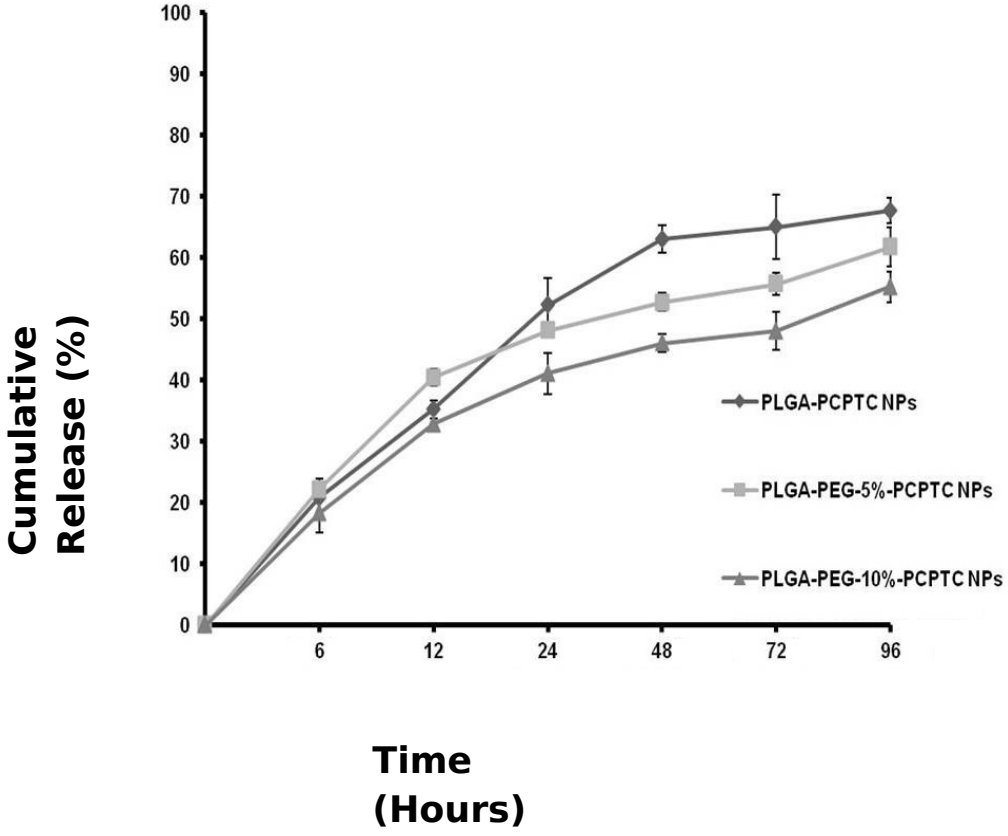

Figure 4

Cumulative release profile of PCPTC-loaded nanoparticles where percentage of payload released was determined on following time intervals (0h, 6h, 12h, 24h, 48h, 72h and 96h, h = hours), (n=3).

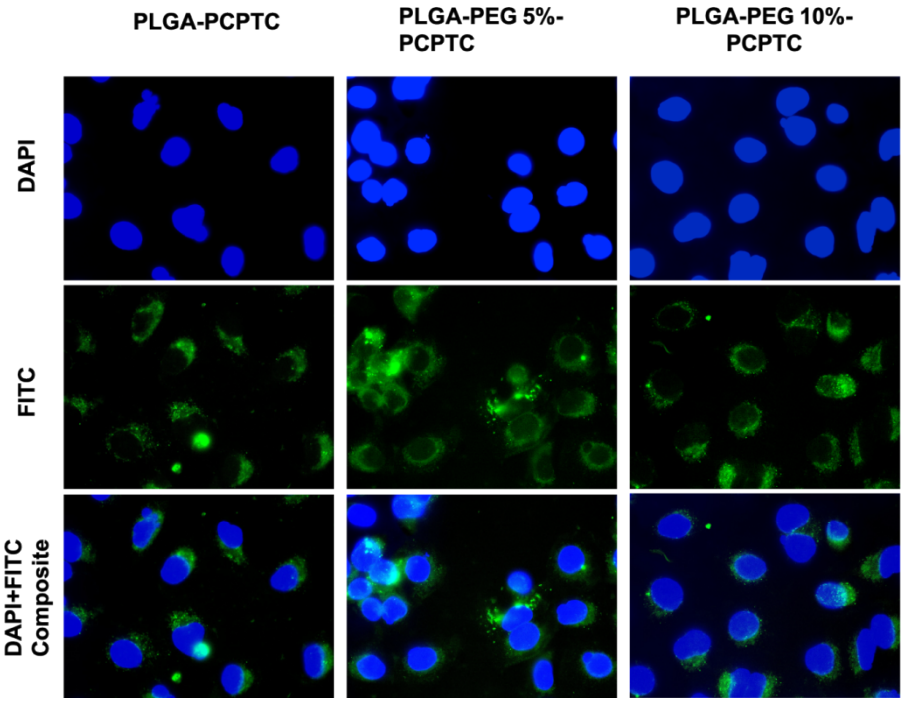

Figure 5

Intracellular localisation of PCPTC-loaded nanoparticles in MDA-MB231 cancer cell line where two channels were used to capture images, i.e., DAPI channel (λ_{ex}-358nm, λ_{em}-461 nm) for visualising blue stained nucleus and FITC (λ_{ex}-488 nm, λ_{em}-519 nm) for visualizing Coumarin-6 loaded- PCPTC-loaded PLGA & PEGylated PLGA NP.

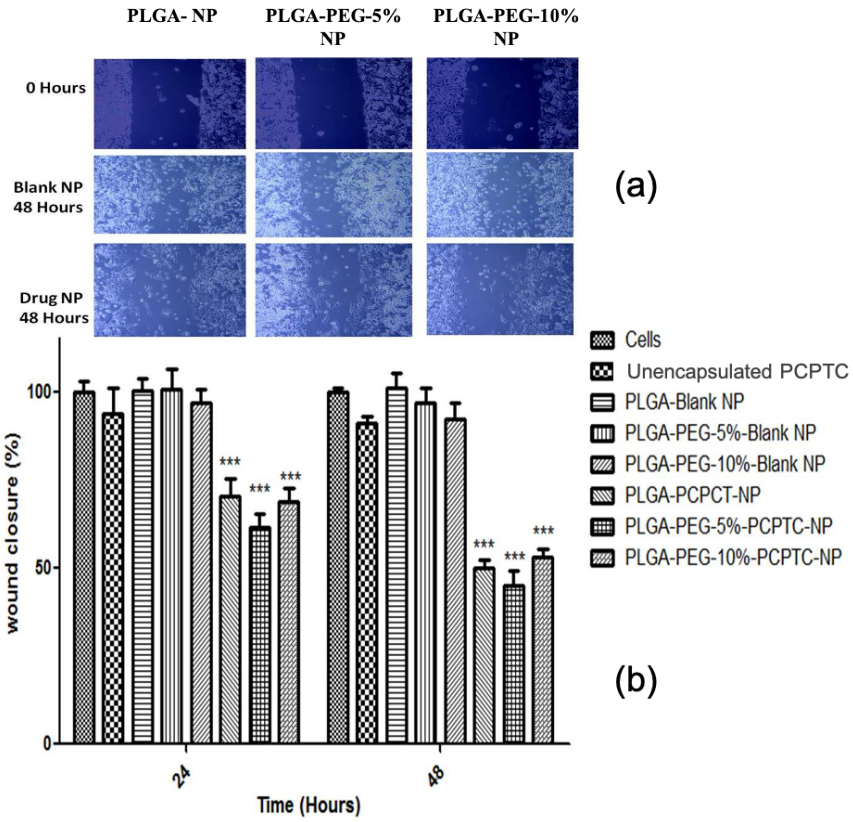

Figure 6

Scratch assay on MDA-MB231 Cell line, (A) microscopic images of effect of PCPTC-loaded NP on cell migration, (B) graphical representation of effect of PCPTC-loaded NP on the rate of migration of MDA-MB231 cells up to 48 hours. PCPTC Concentration used was 2.5 µg ml^{-1}. Values are mean ± SD with n=3. *P<0.05, **P<0.01, ***P<0.001,

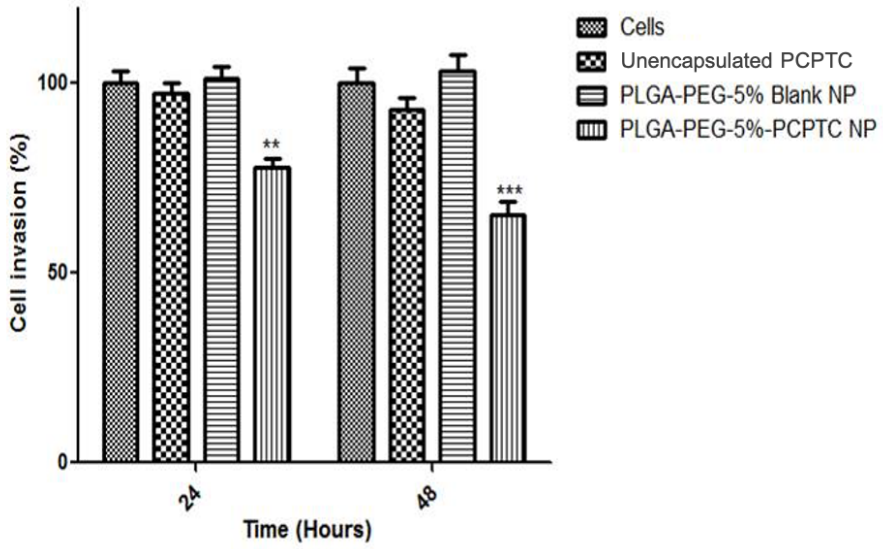

Figure 7

Invasion studies showing the effect of PLGA-PEG-5%-PCPTC NP on invasion of MDA-MB231 cells. Values are mean ± SD with n=3. *P<0.05, **P<0.01, ***P<0.001, where cell invasion reduced by loaded-NP were compared with the cell invasion obtained by blank-NP

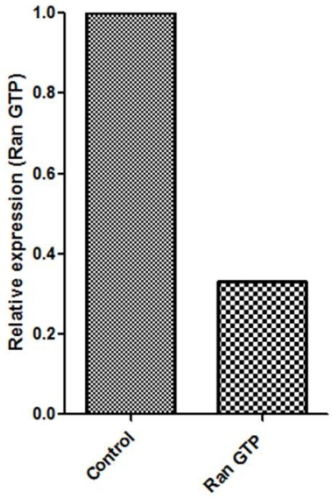

Figure 8

Ran Pull-Down assay result of Ran GTPase in MDA-MB231 cells, Where, Lane 1 is control (supernatant of the cells without treatment), Lane 2 is PLGA-PEG-5%-PCPTC-NP (supernatant of the cells treated with PLGA-PEG-5%-PCPTC NP). The bar graph shows the quantitative reduction of the percentage of active Ran GTP on introduction of PCPTC-NP, the expression of Ran GTP in treated cells were found to be 33.2 % relative to the untreated cells.